Liver-Specific Deletion of Protein-Tyrosine Phosphatase 1B (PTP1B) Improves Metabolic Syndrome and Attenuates Diet-Induced Endoplasmic Reticulum Stress

Mirela Delibegovic,[1,6] Derek Zimmer,[2] Caitlin Kauffman,[2] Kimberly Rak,[2] Eun-Gyoung Hong,[3,4] You-Ree Cho,[4] Jason K. Kim,[3,4] Barbara B. Kahn,[5] Benjamin G. Neel,[1,7] and Kendra K. Bence[2]

OBJECTIVE—The protein tyrosine phosphatase PTP1B is a negative regulator of insulin signaling; consequently, mice deficient in PTP1B are hypersensitive to insulin. Because PTP1B$^{-/-}$ mice have diminished fat stores, the extent to which PTP1B directly regulates glucose homeostasis is unclear. Previously, we showed that brain-specific PTP1B$^{-/-}$ mice are protected against high-fat diet–induced obesity and glucose intolerance, whereas muscle-specific PTP1B$^{-/-}$ mice have increased insulin sensitivity independent of changes in adiposity. Here we studied the role of liver PTP1B in glucose homeostasis and lipid metabolism.

RESEARCH DESIGN AND METHODS—We analyzed body mass/adiposity, insulin sensitivity, glucose tolerance, and lipid metabolism in liver-specific PTP1B$^{-/-}$ and PTP1Bfl/fl control mice, fed a chow or high-fat diet.

RESULTS—Compared with normal littermates, liver-specific PTP1B$^{-/-}$ mice exhibit improved glucose homeostasis and lipid profiles, independent of changes in adiposity. Liver-specific PTP1B$^{-/-}$ mice have increased hepatic insulin signaling, decreased expression of gluconeogenic genes PEPCK and G-6-Pase, enhanced insulin-induced suppression of hepatic glucose production, and improved glucose tolerance. Liver-specific PTP1B$^{-/-}$ mice exhibit decreased triglyceride and cholesterol levels and diminished expression of lipogenic genes SREBPs, FAS, and ACC. Liver-specific PTP1B deletion also protects against high-fat diet–induced endoplasmic reticulum stress response in vivo, as evidenced by decreased phosphorylation of p38MAPK, JNK, PERK, and eIF2α and lower expression of the transcription factors C/EBP homologous protein and spliced X box-binding protein 1.

CONCLUSIONS—Liver PTP1B plays an important role in glucose and lipid metabolism, independent of alterations in adiposity. Inhibition of PTP1B in peripheral tissues may be useful for the treatment of metabolic syndrome and reduction of cardiovascular risk in addition to diabetes. ***Diabetes*** **58:590–599, 2009**

From the [1]Cancer Biology Program, Beth Israel Deaconess Medical Center and Harvard Medical School, Boston, Massachusetts; the [2]Department of Animal Biology, School of Veterinary Medicine, University of Pennsylvania, Philadelphia, Pennsylvania; the [3]Department of Cellular and Molecular Physiology, Pennsylvania State University College of Medicine, Hershey, Pennsylvania; the [4]Department of Internal Medicine, Section of Endocrinology and Metabolism, Yale University School of Medicine, New Haven, Connecticut; the [5]Division of Endocrinology, Diabetes and Metabolism, Department of Medicine, Beth Israel Deaconess Medical Center and Harvard Medical School, Boston, Massachusetts; the [6]School of Biological Sciences, University of Aberdeen, Aberdeen, U.K.; and the [7]Division of Stem Cell and Developmental Biology, Ontario Cancer Institute, Toronto, Canada.

Corresponding authors: Kendra Bence, kbence@vet.upenn.edu, and Mirela Delibegovic, m.delibegovic@abdn.ac.uk.

Received 9 July 2008 and accepted 8 December 2008.

Published ahead of print at http://diabetes.diabetesjournals.org on 15 December 2008. DOI: 10.2337/db08-0913.

In response to nutrients, insulin is secreted from pancreatic β-cells directly into the portal circulation, where it promotes the storage of energy in the fed state and is the major regulator of glucose homeostasis (1,2). Insulin affects many components of hepatic carbohydrate and lipid metabolism, including glycogen synthesis, lipogenesis, and gluconeogenesis. These effects are achieved by modification of key molecular targets, either by reversible phosphorylation or by alteration of gene expression. Insulin promotes the expression of genes encoding glycolytic and lipogenic enzymes and suppresses genes encoding gluconeogenic enzymes (3).

Insulin action is mediated by insulin receptors (IRs) on the plasma membranes of responsive cells (4). Activation of the IRs leads to transphosphorylation of tyrosine residues in the IR activation loop, which in turn leads to the enhanced ability of the IRs to phosphorylate target proteins, such as insulin receptor substrates (IRSs). Tyrosyl phosphorylated IRS proteins act as docking sites for several SH2 domain-containing proteins, including the p85 regulatory subunit of phosphatidylinositol 3-kinase. Phosphatidylinositol 3-kinase becomes activated upon binding to IRS proteins, and its phosphoinositide products facilitate the activation of downstream targets.

Metabolic syndrome, type 2 diabetes, and cardiovascular disease are complex disorders that are associated with obesity, aging, sedentary lifestyle, and genetic predisposition. A common feature of these disorders is the development of insulin resistance, resulting in decreased insulin-stimulated glucose uptake, failure to suppress hepatic glucose production, and accumulation of hepatic lipid. Although the detailed mechanism(s) underlying insulin resistance remain controversial (4–7), there is general agreement that impaired post-IR signaling is involved (8).

Recent data suggest that prolonged high-fat feeding in mice leads to increased endoplasmic reticulum (ER) stress in liver and adipose tissue and contributes to the development of insulin resistance (9). The ER is a site of secretory and membrane protein synthesis and modification (10). Upon disruption in either protein folding or modification within the ER, the unfolded protein response (UPR) is activated. The unfolded protein response activates signaling through three stress-sensing proteins found on the ER membrane: PKR-like eukaryotic initiation factor 2α kinase (PERK), inositol-requiring kinase-1α (IRE-1α), and activat-

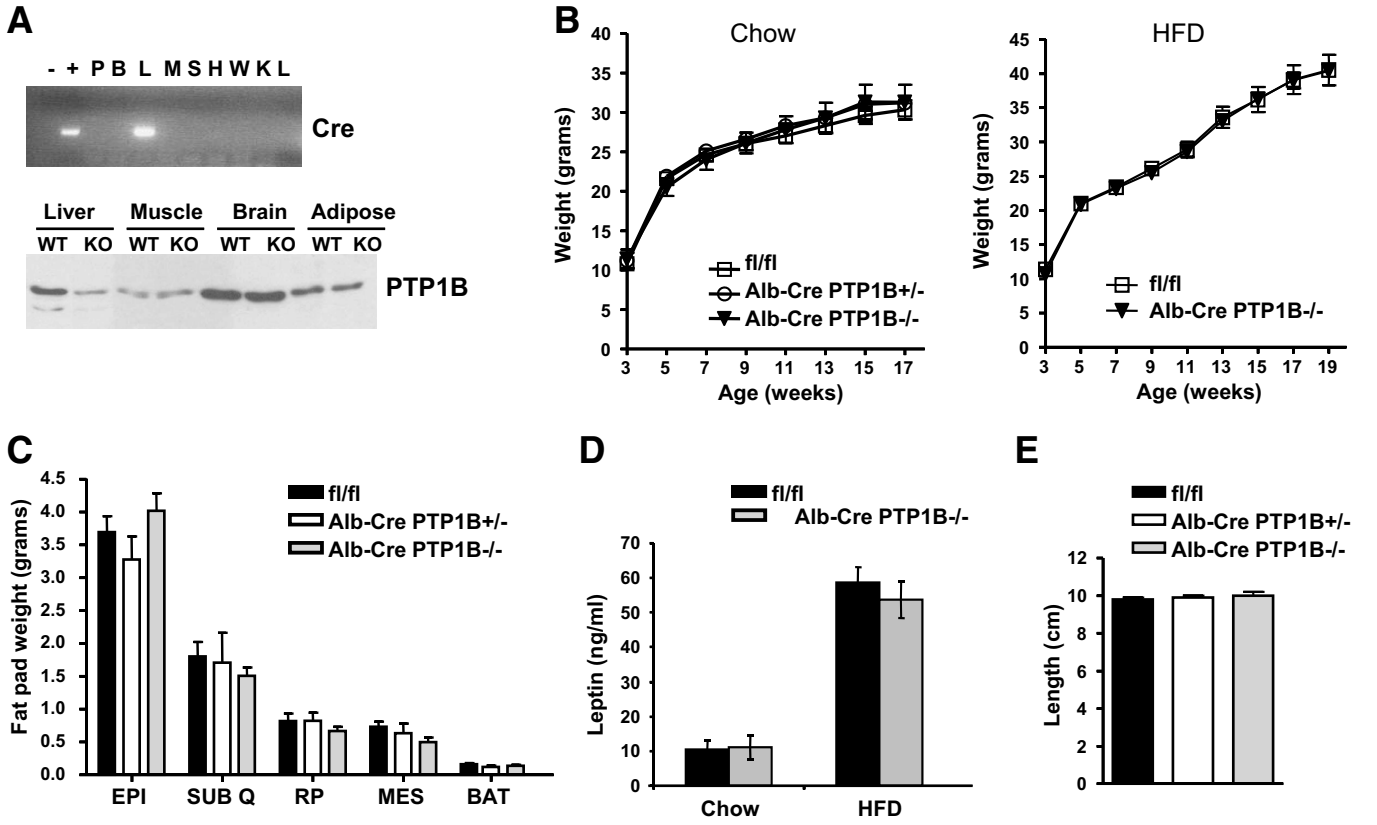

FIG. 1. Liver-specific PTP1B deletion has no effect on body weight or adiposity. *A*: Deletion efficiency, as detected by PCR and Western blotting, in the indicated tissues from Alb-Cre-PTP1B$^{-/-}$ and fl/fl littermates. PCR was performed on DNA isolated from Alb-Cre-PTP1B$^{-/-}$ tissues: P, pituitary; B, brain; L, liver; M, gastrocnemius muscle; S, spleen; H, heart; W, abdominal white adipose tissue; K, kidney; and L, lung. "−" and "+" represent negative and positive controls, respectively. The immunoblot in the *lower panel* indicates ~80% deletion of PTP1B protein in liver, consistent with deletion from hepatocytes, which comprise that approximate percentage of the liver. *B*: Weight curves for Alb-Cre-PTP1B$^{-/-}$ (n = 6) and Alb-Cre-PTP1B$^{+/-}$ mice (n = 10) vs. fl/fl controls (n = 16) on chow diet from weaning to 17 weeks of age (*left*). Weight curves for Alb-Cre-PTP1B$^{-/-}$ (n = 12) and fl/fl controls (n = 12) on HFD from weaning to 19 weeks of age (*right*). *C*: Fat pad weights of 19-week-old Alb-Cre-PTP1B$^{-/-}$ (n = 12) and Alb-Cre-PTP1B$^{+/-}$ (n = 9) vs. fl/fl mice (n = 12) on HFD. BAT, brown adipose tissue; EPI, epididymal; MES, mesenteric; RP, retroperitoneal; and SUB Q, subcutaneous. *D*: Leptin levels (ng/ml) in Alb-Cre-PTP1B$^{-/-}$ (n = 5) and fl/fl mice (n = 9) on chow diet and Alb-Cre-PTP1B$^{-/-}$ (n = 10) and fl/fl mice (n = 12) on HFD (at 5 months of age). *E*: Length (cm) of Alb-Cre-PTP1B$^{-/-}$ (n = 12) and PTP1B$^{+/-}$ (n = 9) vs. fl/fl mice (n = 12) on HFD.

ing transcription factor-6 (ATF-6) (11,12). The main purpose of the UPR is to counter the deleterious effects of ER stress, since prolongation of the ER stress response leads to apoptosis, inflammation, and hepatic lipid accumulation (13).

Whole-body knockout studies of protein tyrosine phosphatase 1B (PTP1B) in mice established PTP1B as a key regulator of body mass and insulin sensitivity (14,15). PTP1B$^{-/-}$ mice are lean because of enhanced leptin sensitivity, are more insulin sensitive, and have enhanced muscle and liver IR phosphorylation. In addition, PTP1B$^{-/-}$ primary and immortalized fibroblasts exhibit decreased ER stress response through impaired IRE1 signaling, but the in vivo relevance of these observations is not clear (16).

We recently generated tissue-specific PTP1B$^{-/-}$ mice and found the brain to be the primary site mediating the effects of PTP1B on body mass. Because mice with global PTP1B deficiency and brain-specific PTP1B$^{-/-}$ mice are lean, and leanness improves insulin sensitivity, it has been difficult to assess the direct role of PTP1B in insulin sensitivity. Furthermore, recent studies have implicated a brain-liver circuit in regulating insulin sensitivity, raising the possibility that peripheral insulin sensitivity may be mediated partly via neuronal circuits (17). Indeed, young female brain-specific PTP1B$^{-/-}$ mice are more insulin sensitive than controls, despite having comparable body weight (18).

These studies raised the possibility that all of the insulin sensitivity seen in PTP1B$^{-/-}$ mice might be due to central effects. To begin to address this issue, we generated muscle-specific PTP1B$^{-/-}$ mice and found that, compared with controls, these mice exhibit significant improvement in whole-body glucose homeostasis on both chow and high-fat diet (HFD) despite comparable body weight and adiposity (19). In light of the critical role of the liver in glucose homeostasis and the pathogenesis of diabetes (5,13), and the potential role of PTP1B in the ER stress response (16), we asked whether PTP1B also has autonomous effects on hepatic control of glucose homeostasis and lipid metabolism by generating liver-specific PTP1B$^{-/-}$ mice.

RESEARCH DESIGN AND METHODS

Animal studies. PTP1B floxed mice were generated previously (18). Alb-Cre mice on a 129Sv/C57Bl6 hybrid background were obtained from C. Ronald Kahn (Joslin Diabetes Center). All mice studied were age-matched littermate males on the mixed 129Sv/C57Bl6 background. Mice were maintained in a temperature-controlled barrier facility on a 12-h light/dark cycle with free access to water and food (19). Genotyping for the PTP1B floxed allele and the presence of Cre was performed by PCR (18).

Body composition. Mice were placed on standard lab chow or HFD at weaning (21 days old), and weights were monitored weekly. Length was

TABLE 1
Blood glucose, serum insulin, plasma free fatty acids, and liver glycogen were analyzed in male PTP1B fl/fl control and Alb-Cre-PTP1B$^{-/-}$ mice (n = 6–18 mice/group) fed chow or HFD as indicated

	Chow		HFD	
	PTP1B fl/fl (control)	Alb-Cre-PTP1B$^{-/-}$	PTP1B fl/fl (control)	Alb-Cre-PTP1B$^{-/-}$
Blood glucose (mg/dl)				
Fasted 8 weeks	55.4 ± 2.5	55.0 ± 1.7	75.0 ± 4.3	63.2 ± 5.7
Fed 8 weeks	111.1 ± 4.6	111.6 ± 2.2	111.6 ± 3.9	88.1 ± 2.3*
Fasted 16 weeks	70.8 ± 5.5	63.6 ± 4.9	72.4 ± 6.6	50.2 ± 7.3†
Fed 16 weeks	103.7 ± 4.6	94.8 ± 3.3	121.2 ± 5.5	110.5 ± 7.3
Serum insulin (ng/ml)				
Fed 8 weeks	0.64 ± 0.10	0.64 ± 0.08	1.30 ± 0.31	1.06 ± 0.15
Fed 16 weeks	ND	ND	5.11 ± 1.11	2.35 ± 0.24*
Pre-clamp (fasted)	0.20 ± 0.05	0.13 ± 0.02	ND	ND
Clamp	0.93 ± 0.18	0.72 ± 0.18		
GTT time 0 min	0.30 ± 0.06	0.24 ± 0.06		
GTT time 15 min	0.59 ± 0.08	0.73 ± 0.08		
GTT time 30 min	0.54 ± 0.07	0.63 ± 0.04		
Plasma free fatty acids (mmol/l)				
Fasted 16 weeks	ND	ND	0.885 ± 0.075	0.942 ± 0.079
Fed 16 weeks	0.456 ± 0.047	0.413 ± 0.067	0.523 ± 0.041	0.483 ± 0.065
Liver glycogen (μg/mg)				
Fasted	ND	ND	2.16 ± 0.44	1.94 ± 0.63
Fed			19.92 ± 1.22	20.91 ± 0.58

Data are means ± SE and were analyzed by two-tailed Student's t test. *$P < 0.01$, †$P < 0.05$ for the indicated genotype compared with PTP1B fl/fl control littermates. ND, not determined.

measured from nose to rump (cm). Fat pads were dissected from mice fed an HFD for 18 weeks and weighed individually (19).

Metabolic measurements. Glucose in tail blood was assayed using a glucometer (Lifescan). Fed measurements were taken between 8:00 and 10:00 A.M. and, where indicated, from mice fasted for 12 h. Serum insulin and leptin were determined by ELISA (CrystalChem), and free fatty acids were quantified by enzymatic assay (Wako). Insulin tolerance tests (ITTs) and glucose tolerance tests (GTTs) were performed as described (18,19). A 2-h hyperinsulinemic-euglycemic clamp was conducted in awake Alb-Cre-PTP1B$^{-/-}$ mice (n = 15) and fl/fl littermates (n = 13) at a continuous insulin infusion rate of 2.5 mU · kg^{-1} · min^{-1}, as described previously (19 and in the supplemental information, found in an online-only appendix at http://diabetes.diabetesjournals.org/cgi/content/full/db08-0913/DC1).

Biochemical studies. For insulin signaling experiments, animals were fasted for 12 h, saline or insulin (10 mU/g) was injected intraperitoneally, and livers were removed 10 min later. Mouse tissues were dissected and frozen in liquid N_2. Tissue lysates were prepared by extraction in radioimmunoprecipitation assay (RIPA) buffer at 4°C, followed by clarification at 14,000g (19,20). For immunoblots, proteins were resolved by SDS-PAGE and transferred to PVDF. Immunoblots were performed with polyclonal antibodies against pIR1162/1163 (Invitrogen), IRβ (Santa Cruz), IRS-1/IRS-2 (Millipore), p85 (Millipore), phospho-GS-Ser641 (Cell Signaling), glycogen synthase chicken antibody (gift from the late Dr. John Lawrence, UVA), or PTP1B (Millipore). For ER stress experiments, the following antibodies, all from Cell Signaling, were used: p-p38, p38, pJNK, pPERK, peIF2a (Ser 51), and eIF2α. Proteins were visualized using enhanced chemiluminescence and quantified by scanning densitometry (Image J software). Phosphorylated IRS-1 in livers (2 μg protein) was detected by enzyme-linked immunosorbent assay (ELISA) (PathScan Phospho-IRS-1, Cell Signaling). For immunoprecipitation studies, IRS-1 or IRS-2 was immunoprecipitated from liver lysates (1 mg) with IRS-1 (Millipore) or IRS-2 antibody (Santa Cruz) and protein A Sepharose. Immunoprecipitates were washed four times with lysis buffer, subjected to SDS-PAGE, transferred to PVDF membranes, and immunoblotted with anti-phosphotyrosine antibody (Santa Cruz) or p85 antibody (Millipore). No differences in total IRS-1 or IRS-2 levels were detected.

Gene expression analysis. Liver RNA was isolated using Trizol (Invitrogen) and purified with the RNeasy kit (Qiagen). A total of 1 μg RNA was reverse-transcribed in 20 μl reaction volume with the Advantage RT-for-PCR kit (Clontech). Then 1–2 μl cDNA was used to amplify the target genes in the real-time RT-PCR (20 μl) using SYBR Green PCR Master Mix (ABI) followed by analysis using the Eppendorf Mastercycler ep Realplex. Relative gene expression was calculated using the comparative Ct ($2^{-\delta\delta Ct}$) method. The relative copy number of GAPDH and 18S was used for normalization (SABiosciences RT^2 qPCR Primer Assays). PCRs were followed by melting curve (60–95°C) and agarose gel analysis to ensure specificity (for primer sequences and PCR conditions, see the supplemental information).

Lipid analysis. Serum and liver triglycerides and cholesterol were measured at the Vanderbilt MMPC Lipid Core facility. Lipids were extracted using the method of Folch et al. (21), and individual lipid classes were separated by thin-layer chromatography and visualized by rhodamine 6G. Triglycerides were quantified as described (22). Cholesterol measurements were performed by gas chromatography as described (23).

RESULTS

Generation of liver-specific PTP1B$^{-/-}$ mice. Mice with liver-specific PTP1B deletion were generated by crossing PTP1Bfl/fl mice to mice expressing Cre recombinase under the control of the albumin promoter (Alb-Cre). The resultant Alb-Cre PTP1B +/fl mice were crossed to PTP1Bfl/fl mice, yielding Alb-Cre PTP1Bfl/fl mice (hereafter termed Alb-Cre-PTP1B$^{-/-}$ mice), Alb-Cre PTP1B +/fl mice, and PTP1Bfl/fl controls (18). PCR for the deleted PTP1B allele confirmed that deletion occurred only in the liver (Fig. 1*A*, *top panel*). As expected, Alb-Cre-PTP1B$^{-/-}$ mice exhibited ~80% reduction in PTP1B protein in the liver (1), consistent with hepatocyte-specific deletion. Other insulin-responsive tissues had normal levels of PTP1B protein (Fig. 1*A*, *bottom panel*).

Alb-Cre-PTP1B$^{-/-}$ and control mice were weaned onto either HFD (55% kcal from fat) or normal chow (4.5% fat). The absence of PTP1B in hepatocytes had no effect on body weight on either diet (Fig. 1*B*), as expected from previous studies (18). Adiposity, as assessed by fat pad weights (Fig. 1*C*) and leptin levels (Fig. 1*D*), and length (Fig. 1*E*), were unaffected by PTP1B deficiency. Hematoxylin and eosin staining of liver sections revealed no overt histological differences between Alb-Cre-PTP1B$^{-/-}$ and fl/fl control littermates (data not shown).

Improved glucose homeostasis in Alb-Cre-PTP1B$^{-/-}$ mice. Compared with littermate controls, Alb-Cre-PTP1B$^{-/-}$ mice fed an HFD exhibited lower fed glucose levels at 8 weeks of age and lower fasted glucose, serum

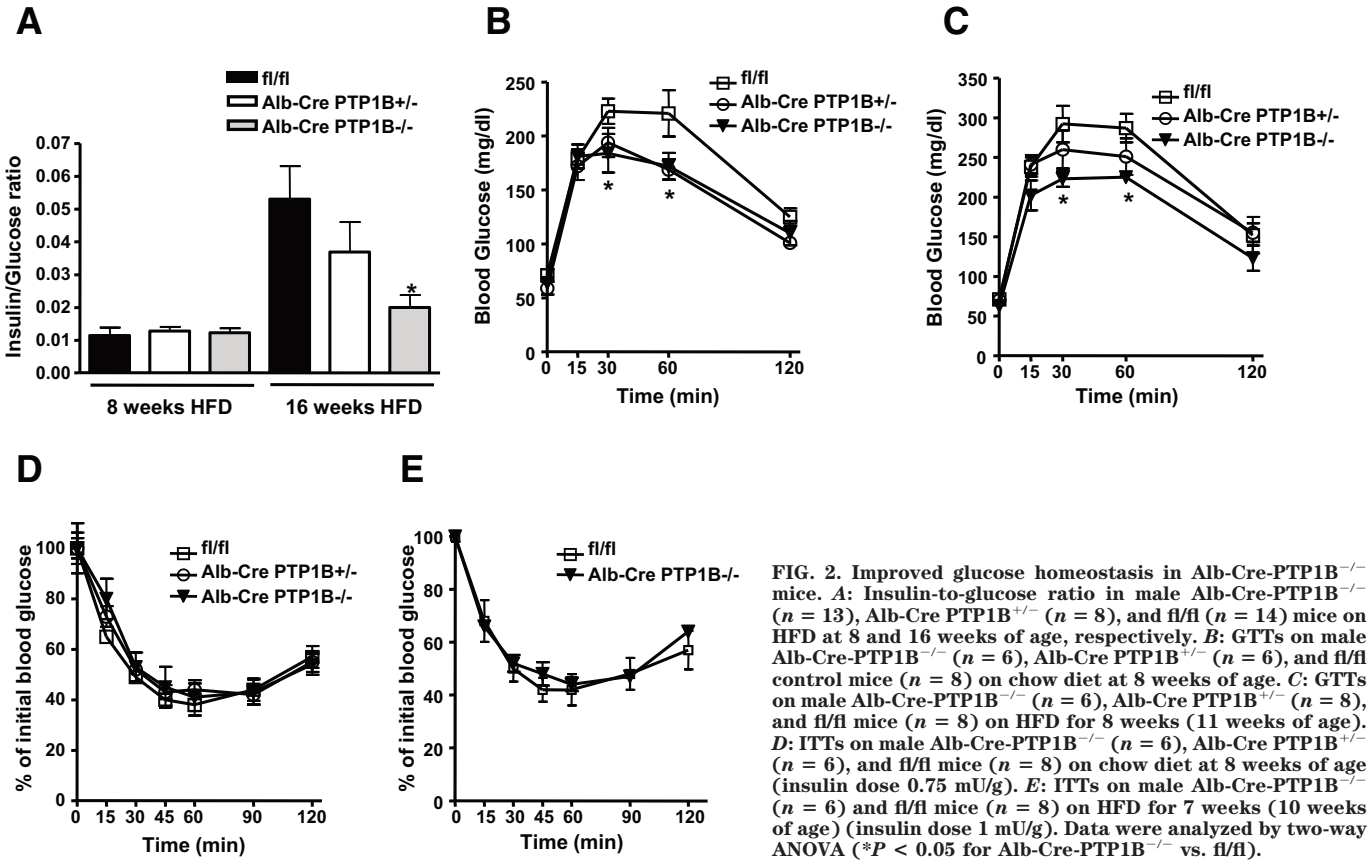

FIG. 2. Improved glucose homeostasis in Alb-Cre-PTP1B$^{-/-}$ mice. *A*: Insulin-to-glucose ratio in male Alb-Cre-PTP1B$^{-/-}$ (n = 13), Alb-Cre PTP1B$^{+/-}$ (n = 8), and fl/fl (n = 14) mice on HFD at 8 and 16 weeks of age, respectively. *B*: GTTs on male Alb-Cre-PTP1B$^{-/-}$ (n = 6), Alb-Cre PTP1B$^{+/-}$ (n = 6), and fl/fl control mice (n = 8) on chow diet at 8 weeks of age. *C*: GTTs on male Alb-Cre-PTP1B$^{-/-}$ (n = 6), Alb-Cre PTP1B$^{+/-}$ (n = 8), and fl/fl mice (n = 8) on HFD for 8 weeks (11 weeks of age). *D*: ITTs on male Alb-Cre-PTP1B$^{-/-}$ (n = 6), Alb-Cre PTP1B$^{+/-}$ (n = 6), and fl/fl mice (n = 8) on chow diet at 8 weeks of age (insulin dose 0.75 mU/g). *E*: ITTs on male Alb-Cre-PTP1B$^{-/-}$ (n = 6) and fl/fl mice (n = 8) on HFD for 7 weeks (10 weeks of age) (insulin dose 1 mU/g). Data were analyzed by two-way ANOVA (*P < 0.05 for Alb-Cre-PTP1B$^{-/-}$ vs. fl/fl).

insulin levels, and insulin-to-glucose ratios at ~16 weeks of age, indicating an overall improvement in glucose homeostasis (Table 1; Fig. 2*A*). Alb-Cre-PTP1B$^{-/-}$ mice also exhibited an enhanced ability to clear glucose from the peripheral circulation during intraperitoneal GTTs on either chow (8 weeks of age) or HFD (11 weeks of age) compared with controls (Fig. 2*B* and *C*). Insulin secretion during the GTTs was similar in Alb-Cre-PTP1B$^{-/-}$ and fl/fl controls (Table 1). In contrast to their improved GTTs, ITTs were normal in Alb-Cre-PTP1B$^{-/-}$ mice (Fig. 2*D* and *E*; see DISCUSSION).

Increased suppression of hepatic glucose production in Alb-Cre-PTP1B$^{-/-}$ mice. To assess whether improved glucose tolerance was due to autonomous effects of PTP1B deficiency in the liver, we performed hyperinsulinemic-euglycemic clamps in male Alb-Cre-PTP1B$^{-/-}$ and fl/fl control mice fed a chow diet. Hepatic glucose production during the insulin-stimulated state (clamp) was significantly lower in Alb-Cre-PTP1B$^{-/-}$ mice (Fig. 3*A*), resulting in ~30% higher insulin-mediated suppression of hepatic glucose production in Alb-Cre-PTP1B$^{-/-}$ mice (Fig. 3*B*). Basal blood glucose levels in Alb-Cre-PTP1B$^{-/-}$ mice were similar to those in control littermates and were maintained at levels comparable to those of controls during the clamp (Fig. 3*C*). The glucose infusion rate required to maintain euglycemia during clamps trended higher in Alb-Cre-PTP1B$^{-/-}$ mice (P = 0.052), indicating an overall improvement in insulin sensitivity (Fig. 3*D*). Insulin-stimulated whole-body glucose turnover and glucose metabolism in skeletal muscle were similar between the two groups (Fig. 3*E–G*). These data suggest that improvement in whole-body glucose homeostasis, as measured by GTT in Alb-Cre-PTP1B$^{-/-}$ mice, is mostly due to increased insulin sensitivity in liver.

Increased insulin signaling in liver lacking PTP1B. To investigate the molecular mechanism of improved hepatic insulin sensitivity in Alb-Cre-PTP1B$^{-/-}$ mice, we injected fasted, male Alb-Cre-PTP1B$^{-/-}$, or fl/fl littermate control mice with insulin or saline (control) and examined insulin signaling in liver. We analyzed phosphorylation of Y1162/Y1163 on the insulin receptor because these sites are reported to be preferentially dephosphorylated by PTP1B (24,25). Insulin-stimulated IR phosphorylation was higher in Alb-Cre-PTP1B$^{-/-}$ mice on a chow diet compared with controls (Fig. 4*A*). High-fat feeding blunted hepatic insulin signaling in fl/fl mice, resulting in a less robust increase in insulin-induced IR phosphorylation. However, insulin-induced IR phosphorylation in Alb-Cre-PTP1B$^{-/-}$ liver was greater than in control mice (Fig. 4*B*). Basal IRS-1 tyrosine phosphorylation was increased in HFD-fed Alb-Cre-PTP1B$^{-/-}$ mice (Fig. 4*C*). Insulin-stimulated IRS-1 phosphorylation tended to be higher in Alb-Cre-PTP1B$^{-/-}$ mice, although this did not reach statistical significance. In contrast, basal tyrosine phosphorylation of IRS-2 was similar between the two groups, but insulin-stimulated IRS-2 phosphorylation was elevated in HFD-fed Alb-Cre-PTP1B$^{-/-}$ mice (Fig. 4*D*). Improved hepatic insulin signaling was also evident downstream, since Alb-Cre-PTP1B$^{-/-}$ mice exhibited higher insulin-stimulated IRS-1 and IRS-2 p85 association than controls, as well as reduced phosphorylation of glycogen synthase (Fig. 4*E*). These biochemical data suggest that the improved hepatic insulin action in Alb-Cre-PTP1B$^{-/-}$ mice is the direct result of increased IR signaling.

Insulin regulates hepatic glucose metabolism in part by altering gene expression (8). Consistent with their improved glucose homeostasis, the levels of peroxisome proliferator–activated receptor-γ coactivator-1α (PGC-

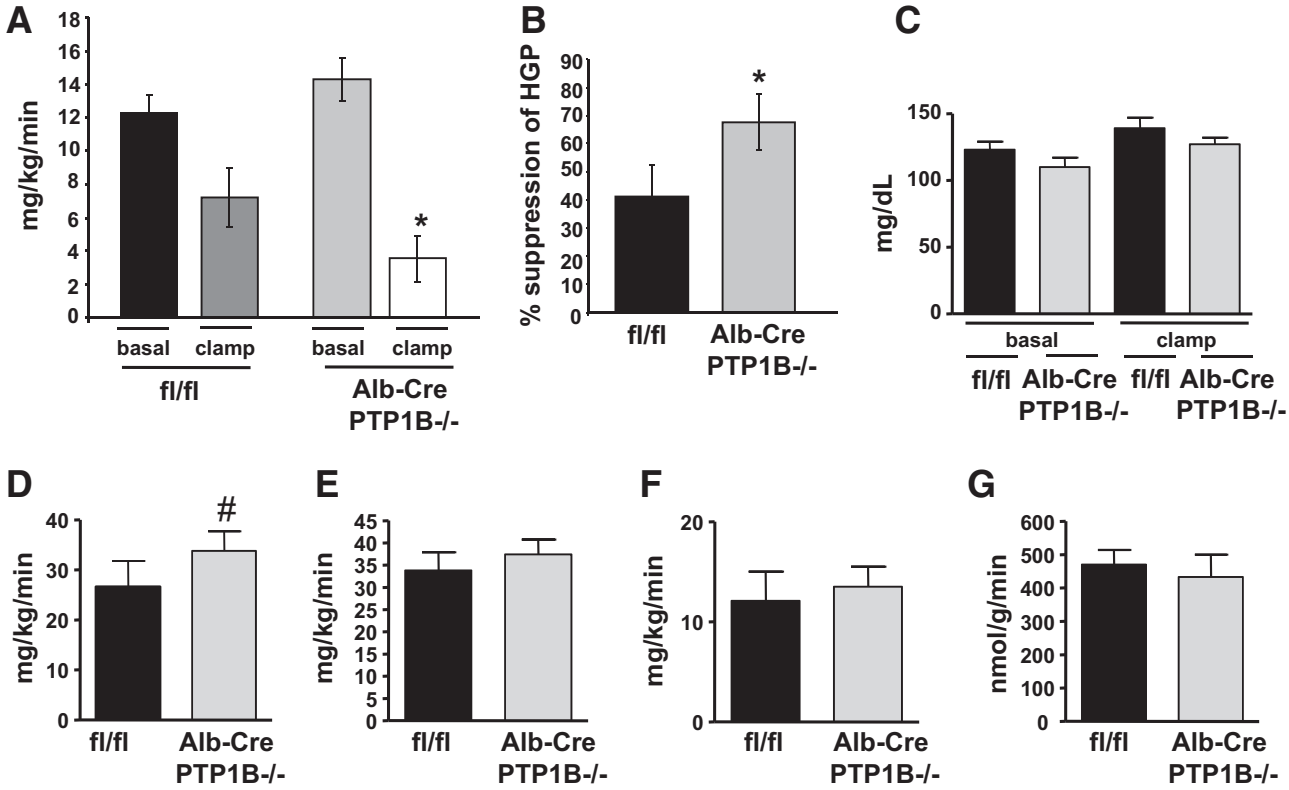

FIG. 3. Hyperinsulinemic-euglycemic clamp studies. Alb-Cre-PTP1B$^{-/-}$ (n = 15) and fl/fl control (n = 13) mice on chow diet at 18–20 weeks of age were subjected to hyperinsulinemic-euglycemic clamp studies (see RESEARCH DESIGN AND METHODS). *A*: Hepatic glucose production. *B*: Hepatic insulin action (percent suppression of hepatic glucose production). *C*: Basal and clamp blood glucose levels. *D*: Whole-body glucose infusion rate. *E*: Whole-body glucose turnover. *F*: Whole-body glycogen and lipid synthesis. *G*: Glucose uptake into gastrocnemius muscle. Results are mean ± SE. Data were analyzed by one-tailed Student's t test (*$P < 0.05$; #$P = 0.052$).

1α), phosphoenolpyruvate carboxykinase (PEPCK), and glucose-6-phosphatase (G-6-Pase) mRNA were significantly lower in Alb-Cre-PTP1B$^{-/-}$ mice fed an HFD for 18 weeks compared with controls (Fig. 4*F*).

Improved lipid homeostasis in Alb-Cre-PTP1B$^{-/-}$ mice. Because the liver plays a major role in lipid metabolism, we assessed several parameters of whole-body lipid homeostasis in Alb-Cre-PTP1B$^{-/-}$ and control mice. Serum free fatty acids were unchanged between the two groups of mice (Table 1). However, liver triglyceride levels were significantly lower in Alb-Cre-PTP1B$^{-/-}$ mice after 5 weeks of high-fat feeding (Fig. 5*A*), whereas this difference was not detectable at 18 weeks of HFD, probably due to very high levels of triglyceride at this time. Serum triglyceride levels were also lower in Alb-Cre-PTP1B$^{-/-}$ mice fed an HFD (Fig. 5*B*).

Lipid homeostasis in vertebrate cells is regulated by a small family of membrane-bound transcription factors, designated sterol regulatory element–binding proteins (SREBPs), which directly activate the expression of >30 genes dedicated to the synthesis and uptake of cholesterol, fatty acids, triglycerides, and phospholipids (26). Analysis of the hepatic lipogenic genes SREBP1a and SREBP1c, and their target genes fatty acid synthase (FAS) and acetyl-CoA carboxylase (ACC), revealed a decrease in their mRNA levels in HFD-fed Alb-Cre-PTP1B$^{-/-}$ mice (Fig. 5*C*). Expression of genes involved in cholesterol synthesis, such as SREBP2 and its target gene 3-hydroxy-3-methylglutaryl-coenzyme A synthase 1 (HMGCS1), also were significantly decreased in HFD-fed Alb-Cre-PTP1B$^{-/-}$ mice (Fig. 5*D*). Consistent with their reduced SREBP2 and HMGCS1 expression, liver cholesterol levels were significantly lower in HFD-fed Alb-Cre-PTP1B$^{-/-}$ mice compared with controls (Fig. 5*E*). In fact, cholesterol levels in Alb-Cre-PTP1B$^{-/-}$ mice fed an HFD were similar to those measured in chow-fed mice (data not shown), suggesting that liver-specific PTP1B deletion protects against cholesterol accumulation caused by prolonged HFD feeding. Serum cholesterol levels in HFD-fed Alb-Cre-PTP1B$^{-/-}$ mice also were lower than in control littermates (Fig. 5*F*).

Decreased ER stress response in HFD-fed Alb-Cre-PTP1B$^{-/-}$ mice. Genetic and dietary obesity in mice induce the ER stress response, which is associated with insulin resistance and intracellular lipid accumulation (9). To investigate whether deficiency of PTP1B in liver protects against HFD-induced ER stress, we analyzed components of the ER stress response in livers of 18-week HFD-fed Alb-Cre-PTP1B$^{-/-}$ and control mice. PTP1B$^{-/-}$ fibroblasts reportedly have decreased phosphorylation of stress-activated p38 MAPK (16). Likewise, Alb-Cre-PTP1B$^{-/-}$ mice had decreased levels of p38 MAPK in their livers, but in addition, JNK, pPERK, and eIF2α phosphorylation was also reduced. Together, these data suggest that Alb-Cre-PTP1B$^{-/-}$ mice are more resistant to HFD-induced ER stress than controls (Fig. 6*A* and *B*). Consistent with this notion, expression of the pro-apoptotic transcription factor C/EBP homologous protein (CHOP), while substantially induced by prolonged high-fat feeding in control and Alb-Cre-PTP1B$^{-/-}$ mice, was significantly lower at the mRNA and protein level in PTP1B-deficient livers (Fig. 6*C*). As expected from in vitro studies (16), expression of XBP1s (a key factor in ER stress) was also reduced (Fig. 6*D*). Thus, mice lacking PTP1B in the liver

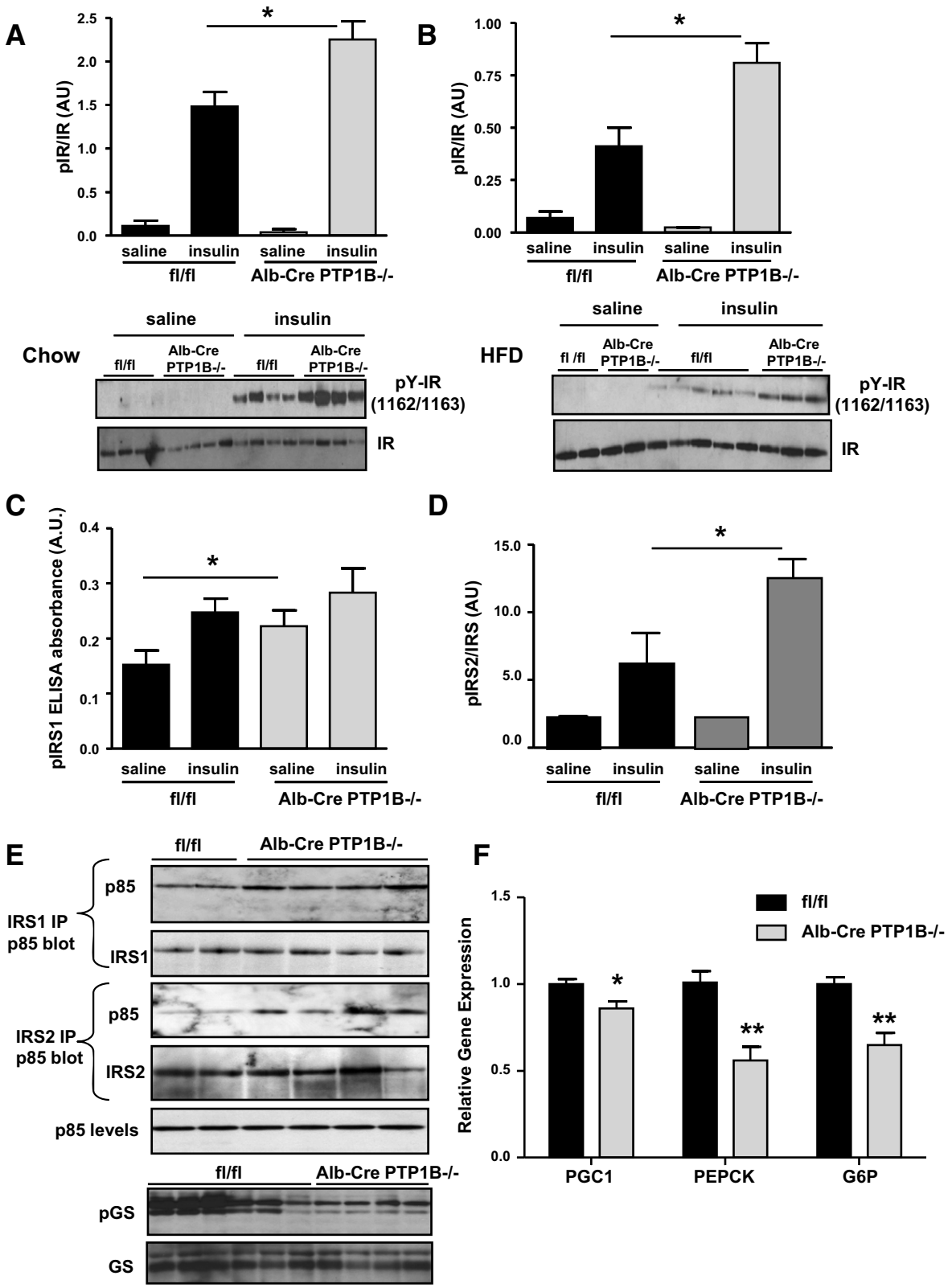

FIG. 4. Enhanced insulin sensitivity in Alb-Cre-PTP1B$^{-/-}$ mice. *A* and *B*: Insulin receptor phosphorylation on Y1162/1163 in livers of 18-week-old male mice on chow (*A*) or HFD (*B*) and injected with saline or insulin (10 mU/g i.p.). *C*: IRS-1 tyrosine phosphorylation in liver as measured by ELISA in 18-week-old mice on HFD. *D*: IRS-2 tyrosine phosphorylation in liver of 18-week-old mice on HFD, quantified by IRS-2 immunoprecipitation and anti-phosphotyrosine immunoblotting. Bar graphs represent pooled, normalized data to total amount of IRS protein (arbitrary units [AU]) from Alb-Cre-PTP1B$^{-/-}$ and fl/fl mice (n = 6–8 per group). Data (*A–D*) were analyzed by one-way ANOVA, followed by a Tukey's multiple comparison test (*$P < 0.05$). *E*: IRS-1 and IRS-2 were immunoprecipitated from liver lysates (18-week-old mice on HFD) and immunoblotted for the p85 regulatory subunit of phosphatidylinositol 3-kinase. Liver lysates from 18-week-old mice on HFD were also immunoblotted for total levels of p85, phospho-glycogen synthase (GS), and glycogen synthase. *F*: Relative expression of PGC1, PEPCK, and G-6-Pase mRNAs, normalized against 18S mRNA levels, measured by quantitative real-time PCR in livers from fasted male Alb-Cre-PTP1B$^{-/-}$ (n = 6) and fl/fl control mice (n = 6) fed HFD for 18 weeks. Results are the means ± SE; data were analyzed using a two-tailed Student's t test (*$P < 0.05$, **$P < 0.01$).

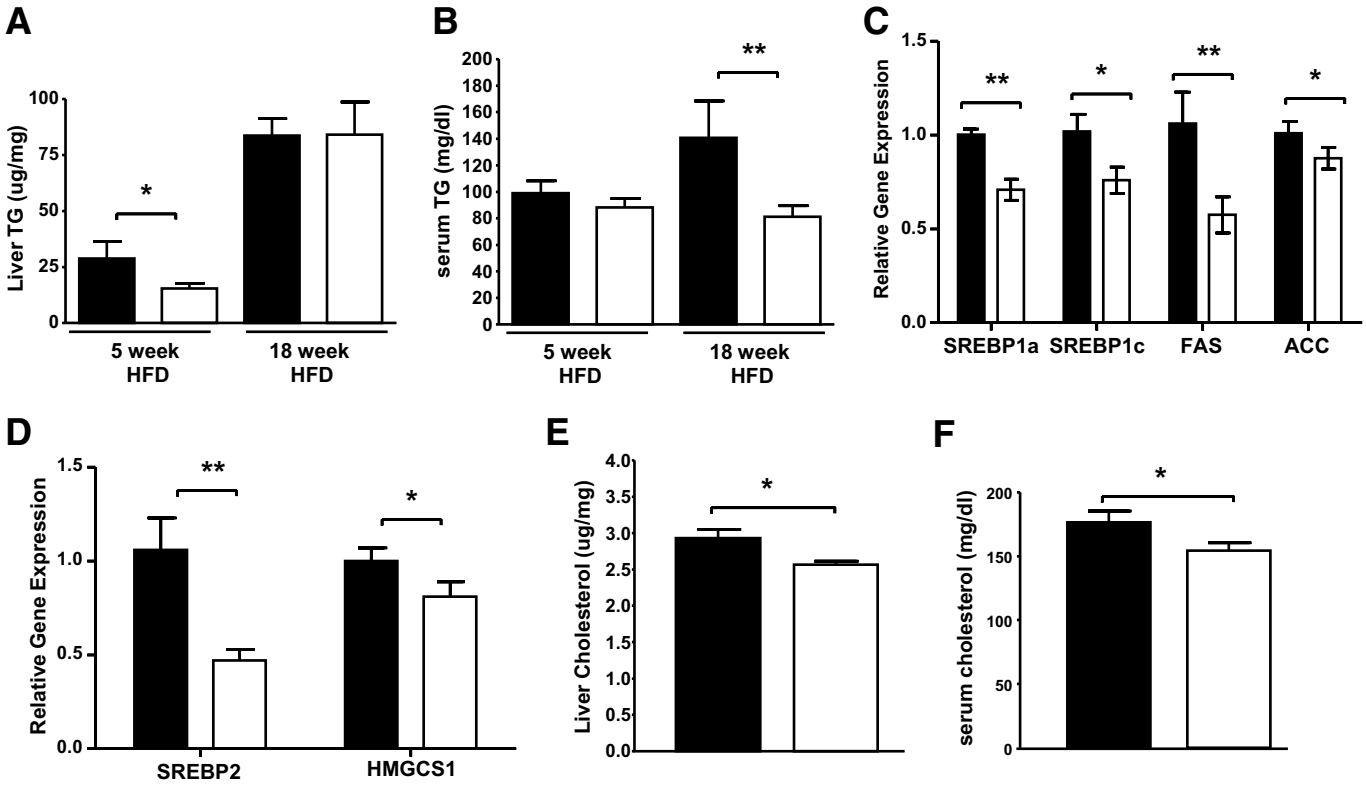

FIG. 5. Improved lipid metabolism in Alb-Cre-PTP1B$^{-/-}$ mice. Liver triglycerides (*A*) or serum triglycerides (*B*) are shown for male Alb-Cre-PTP1B$^{-/-}$ (n = 8) and control (n = 8) mice fed HFD for the indicated time in weeks. *C* and *D*: Relative mRNA levels, measured by quantitative real-time PCR normalized against 18S mRNA, in livers from male Alb-Cre-PTP1B$^{-/-}$ (n = 8) and fl/fl control mice (n = 8) fed HFD for 15 weeks (18 weeks of age) and fasted overnight. Liver (*E*) and serum (*F*) cholesterol in male Alb-Cre-PTP1B$^{-/-}$ (n = 8) and fl/fl control mice (n = 8) on HFD for 15–17 weeks (18–20 weeks of age) is shown. Results represent the means ± SE. Data were analyzed by two-tailed Student's t test (*P < 0.05, **P < 0.01). ■, fl/fl; □, Alb-Cre PTP1B$^{-/-}$.

are more resistant to obesity-induced ER stress, providing an additional potential mechanism by which glucose and lipid homeostasis after prolonged high-fat feeding is improved in these mice.

DISCUSSION

Metabolic syndrome, which is associated with hyperinsulinemia, hyperglycemia, and lipid abnormalities, often leads to diabetes and cardiovascular disease (27–29). Insulin resistance plays a key role in the pathophysiology of metabolic syndrome, resulting in decreased glucose metabolism, insulin action, and alterations in hepatic lipid metabolism. Whole-body knockout studies of mice showed that PTP1B is a major regulator of insulin sensitivity and body weight (14,15) and suggested that PTP1B might be a useful target for the therapy of diabetes and obesity. Here we found that mice lacking PTP1B selectively in the liver have improved glucose homeostasis and reduced levels of triglycerides and cholesterol, independent of changes in body weight or adiposity. These studies show that PTP1B has autonomous effects on both glucose and lipid metabolism in the liver and extend the potential utility of PTP1B inhibitors to the treatment of metabolic syndrome.

The metabolic importance of hepatic insulin signaling was validated by mice with liver-specific deletion of the IR (LIRKO), which exhibit dramatic insulin resistance, severe glucose intolerance, and dysregulated hepatic gene expression (1). Alb-Cre-PTP1B$^{-/-}$ mice exhibit increased insulin-stimulated IR phosphorylation, as well as basal IRS-1 and insulin-stimulated IRS-2 tyrosine phosphorylation. Increased insulin-stimulated IR phosphorylation in these mice is in line with the known role of PTP1B as a negative regulator of IR signaling (14,15), whereas the elevation of basal IRS-1 tyrosine phosphorylation in Alb-Cre-PTP1B$^{-/-}$ mice in the absence of increased basal IR phosphorylation is consistent with previous studies showing that PTP1B also can dephosphorylate IRS-1 directly in vitro (30).

Insulin signaling suppresses gluconeogenic gene expression. Notably, IRS-1 and IRS-2 have complementary roles in the liver, with IRS-1 more closely linked to glucose homeostasis and IRS-2 more important for lipid metabolism (31). Knockdown of IRS-1 in the livers of wild-type mice results in upregulation of G-6-Pase and PEPCK. Consistent with increased IR and IRS-1 tyrosine phosphorylation, we observe decreased expression of G-6-Pase and PEPCK in livers of Alb-Cre-PTP1B$^{-/-}$ mice. The PGC-1α promoter is activated by FoxO1 (32). Insulin suppresses PGC-1α gene expression by promoting Akt phosphorylation and subsequent phosphorylation and nuclear exclusion of FoxO1 (33). PGC-1α expression is elevated in livers of insulin-resistant *ob*/*ob* and LIRKO mice, confirming a key role for insulin as a suppressor of PGC-1 in vivo (34,35). As would be expected in a mouse model with enhanced hepatic insulin sensitivity, we observe decreased expression levels of PGC-1α in livers of Alb-Cre-PTP1B$^{-/-}$ mice.

Alb-Cre-PTP1B$^{-/-}$ mice show enhanced ability of insulin to suppress hepatic glucose production and increased hepatic insulin signaling. Alb-Cre-PTP1B$^{-/-}$ mice also exhibit enhanced ability to clear glucose from the periph-

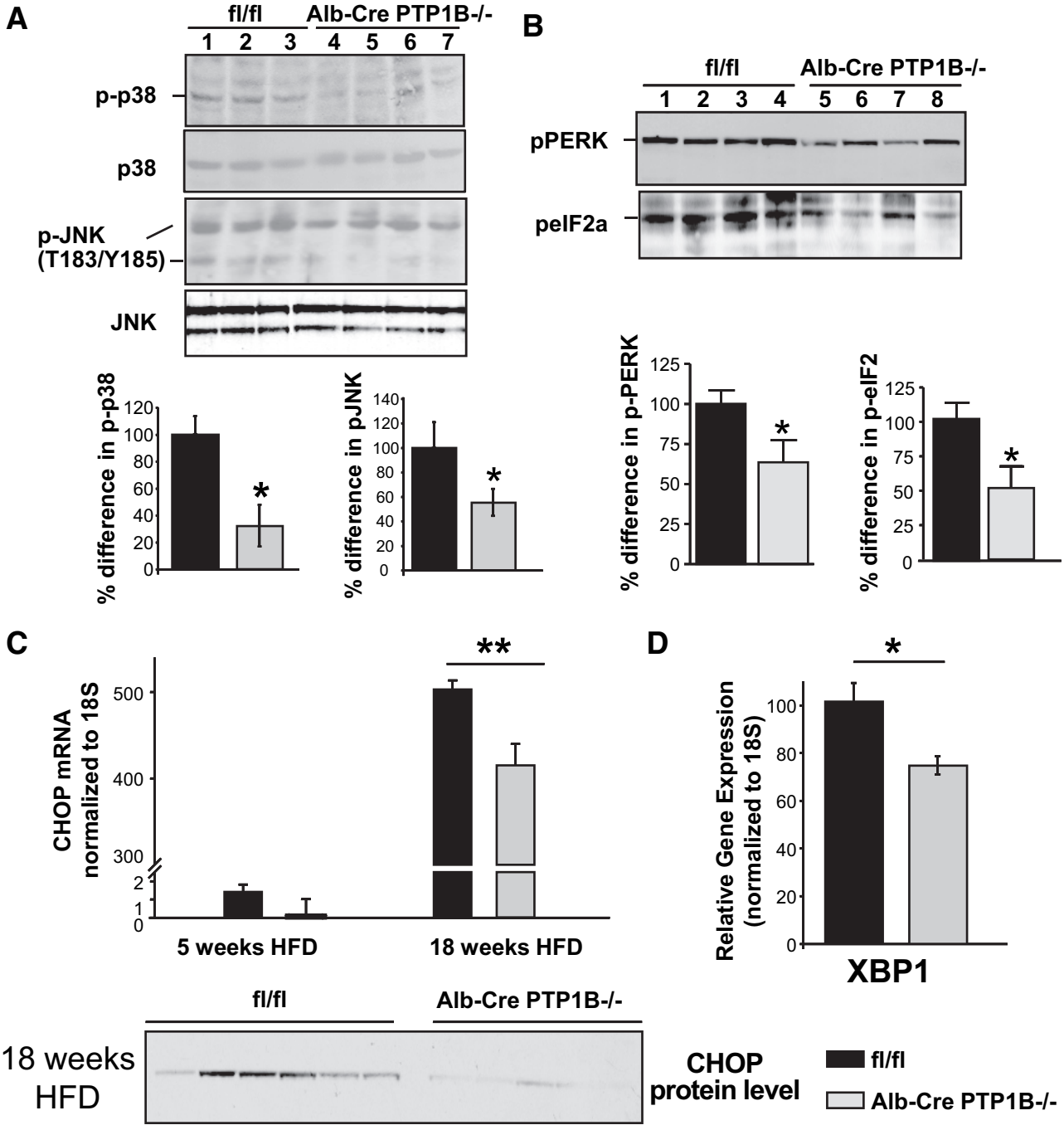

FIG. 6. Alb-Cre-PTP1B$^{-/-}$ mice are resistant to HFD-induced ER stress. *A* and *B*: Liver lysates from mice fed HFD for 18 weeks were analyzed by immunoblotting for p38 MAPK, JNK, PERK, and eIF2α phosphorylation. Blots were stripped and re-probed with total p38 antibodies. JNK, PERK, and eIF2α levels could not be assessed on re-probes, so the same samples were resolved on a parallel gel and immunoblotted for total levels. All immunoblots were quantified by densitometry (Image J). Bar graphs represent pooled data (% difference from control) from Alb-Cre-PTP1B$^{-/-}$ and fl/fl mice. *C*: Expression of CHOP mRNA at 5 and 18 weeks HFD (*C*) XBP1 at 18 weeks HFD (*D*) were measured by quantitative real-time PCR and normalized to 18S expression in livers from Alb-Cre-PTP1B$^{-/-}$ (n = 6) and fl/fl control mice (n = 6). Liver lysates from mice fed HFD for 18 weeks were also analyzed by immunoblotting for total levels of CHOP protein, and these blots are included in *C*. Results represent the means ± SE, and significance was assessed by two-tailed Student's t test (*P < 0.05, **P < 0.01).

eral circulation during GTTs; however, ITTs are similar between Alb-Cre-PTP1B$^{-/-}$ and control mice. Muscle and liver have different "set-points" for insulin action, with higher doses required to stimulate glucose uptake into muscle than to suppress hepatic glucose production. The comparable ITTs in Alb-Cre-PTP1B$^{-/-}$ and control animals are probably due to the relatively high insulin doses used for ITTs, which results in complete suppression of hepatic glucose production.

In addition to its effects on glucose homeostasis, insulin regulates hepatic lipid metabolism by altering lipogenic gene transcription. High insulin levels persistently activate SREBP1c transcription and cleavage, even after patients become "insulin resistant" at the level of gluconeogenesis (26). This leads to increased lipogenic gene expression and accelerated triglyceride accumulation in the liver (36–38). Confirming the importance of the insulin receptor in mediating these effects, LIRKO mice have low serum triglyceride levels and decreased SREBP1c gene expression (29). LIRKO mice, however, also have 10-fold higher

circulating leptin levels (39), and leptin has been suggested to play a role in regulation of glucose homeostasis (40) and plasma triglycerides (41). Surprisingly, SREBP1c and SREBP1a gene expression levels are significantly lower in Alb-Cre-PTP1B$^{-/-}$ mice than in controls. This is opposite to what would be expected from the LIRKO phenotype and the enhanced insulin sensitivity seen in Alb-Cre-PTP1B$^{-/-}$ mice. Consistent with their decreased SREBP1 expression, expression of the SREBP target genes FAS and acetyl-CoA carboxylase and serum triglyceride levels are reduced in Alb-Cre-PTP1B$^{-/-}$ mice. Treatment of *ob/ob* mice with PTP1B oligonucleotides resulted in a similar decrease in lipogenic gene expression, including SREBP1 (38). Furthermore, a study in which high-fructose feeding was used to induce insulin resistance in rats reported a direct association between increased hepatic expression of SREBP1c and PTP1B and suggested a novel mechanism by which PTP1B regulates SREBP1c expression levels by enhancing PP2A activity (43). We therefore suspect that PTP1B may affect SREBP1 gene expression via a pathway distinct from the insulin signaling; however, further work is required to clarify the precise mechanism.

Reduced expression of lipogenic genes in livers of Alb-Cre-PTP1B$^{-/-}$ mice, as well as lower triglyceride, is most likely the direct result of decreased levels of SREBP. Although recent studies of LIRKO mice emphasize the importance of insulin in regulating hepatic lipid balance, for the reasons discussed above, the effects of hepatic PTP1B deficiency on lipid homeostasis cannot be directly attributed to improved insulin action. Previous studies indicate that PTP1B also regulates growth hormone (GH) signaling (44), and GH has been shown to normalize serum triglyceride and cholesterol levels in aged rats (45). We cannot exclude the possibility that hepatic GH signaling may be altered in Alb-Cre-PTP1B$^{-/-}$ mice, although we did not observe differences in linear growth between Alb-Cre-PTP1B$^{-/-}$ and control mice.

Insulin resistance can lead to hepatic fat accumulation, even in the absence of obesity, as evidenced by the prevalence of nonalcoholic fatty liver disease in normal-weight humans. Recent studies have shown that hepatic cholesterol, rather than hepatic triglyceride, may play an important role in the pathogenesis of nonalcoholic fatty liver disease (46). Free cholesterol (but not free fatty acids or triglyceride) accumulation in hepatocytes sensitizes mice to TNF- or Fas-induced fatty liver (47). LIRKO mice fed a high-fat "Western" diet (40% fat) develop marked hypercholesterolemia, whereas consumption of an atherogenic diet (15% fat, 1% cholesterol, 0.5% cholic acid) produces hypercholesterolemia and severe atherosclerosis. Alb-Cre-PTP1B$^{-/-}$ mice have lower expression of genes involved in cholesterol synthesis, including SREBP2 and HMGCS1, as well as decreased serum and liver cholesterol levels on a high-fat diet. High-fat feeding increases PTP1B expression in the liver (48), raising the intriguing possibility that PTP1B deficiency/inhibition in the liver may protect against the progression of fatty liver disease. How liver-specific deficiency of PTP1B results in decreased SREBP2 expression awaits further studies.

Recent studies demonstrated that HFD-feeding and genetic obesity (*ob/ob*) in mice induces the ER stress response (9), leading to cell death, inflammation, insulin resistance, and intracellular lipid accumulation. PERK is an ER transmembrane protein kinase that phosphorylates the α-subunit of eukaryotic translation initiation factor 2 (eIF2α) in response to ER stress, and the phosphorylation status of PERK and eIF2α is therefore a key indicator of ER stress. Examination of downstream markers for ER stress, such as CHOP (13), a b-ZIP transcription factor that potentiates apoptosis (11), or spliced XPB1, which plays a key role in the ER stress response by regulating the transcription of an array of genes, provides an additional readout of these ER stress pathways. Furthermore, ER stress-evoked signaling downstream of IRE1 leads to activation of p38 MAPK and c-Jun NH_2-terminal kinase (JNK) (9).

Studies performed on PTP1B$^{-/-}$ primary and immortalized fibroblasts revealed that the absence of PTP1B protects against ER stress response (16). We found that Alb-Cre-PTP1B$^{-/-}$ livers are more resistant to HFD-induced ER stress response. Phosphorylation of p38 was significantly lower in livers from Alb-Cre-PTP1B$^{-/-}$ mice compared with controls, as was phosphorylation of JNK, PERK, and eIF2α, suggesting that liver PTP1B deficiency causes impaired ER stress–induced IRE1 signaling. CHOP and XBP1s levels also were decreased in HFD-fed Alb-Cre-PTP1B$^{-/-}$ mice, consistent with impaired ER stress-induced PERK signaling. These in vivo studies demonstrate for the first time that PTP1B deficiency affects multiple "arms" of the ER stress response.

Overall, our findings demonstrate that PTP1B plays a critical role in hepatic glucose and lipid metabolism. Selective enhancement of insulin signaling in the liver would normally be expected to suppress gluconeogenesis, while enhancing lipogenesis and fat accumulation in the liver. Alb-Cre-PTP1B$^{-/-}$ mice represent a model of "selective" insulin hypersensitivity, whereby gluconeogenic gene expression is suppressed and glucose homeostasis is improved, whereas triglyceride and cholesterol levels are improved as well. Our previous studies showed that inhibiting neuronal PTP1B is critical for conferring the beneficial effects of PTP1B deficiency on body mass/adiposity (18). Because of technical limitations in designing specific, bioavailable PTP1B inhibitors, the brain may be particularly difficult to target for therapy (49). The current results, combined with our previous studies of muscle-specific PTP1B$^{-/-}$ mice (19), indicate that inhibiting PTP1B in the periphery should result in improved insulin sensitivity. Furthermore, inhibition of PTP1B in liver would have a beneficial lipid-lowering effect. Thus, PTP1B inhibitors may be an attractive therapy for use in the treatment of metabolic syndrome and cardiovascular risk, in addition to insulin resistance and diabetes.

ACKNOWLEDGMENTS

This work was supported by National Institutes of Health (NIH) Grants DK 60838 (to B.B.K. and B.G.N.), DK 60839 (to B.B.K.), R37 CA49152 (to B.G.N.), and U24-DK59635 (to J.K.K.); the Physiology Core Grant DK57521 (to B.B.K.); and a Research Grant from the American Diabetes Association (to B.G.N.). M.D. was the recipient of a postdoctoral fellowship from the American Heart Association and is currently supported by Research Councils UK Fellowship, Diabetes UK project grant, and the Royal Society Research Grant. K.K.B. was supported by a Penn Center for Molecular Studies in Digestive and Liver Disease Pilot Grant (DK50306), University of Pennsylvania Research Foundation, and the USDA (Section 1433 Animal Health

and Disease Formula Grant). Lipid analysis was performed at the Vanderbilt MMPC Lipid Core (DK59637). Parts of this study were performed at the Penn State Mouse Metabolic Phenotyping Center and the Yale Mouse Metabolic Phenotyping Center, and the study was supported by grants from the American Diabetes Association (1-04-RA-47 to J.K.K.) and the Pennsylvania State Department of Health (to J.K.K.).

B.G.N. and B.B.K. have equity in Ceptyr Inc, a company trying to develop PTP1B inhibitors, and B.B.K. also serves on its Scientific Advisory Board. No other potential conflicts of interest relevant to this article were reported.

We thank C. Ronald Kahn (Joslin Diabetes Center) for the Alb-Cre mice.

REFERENCES

1. Michael MD, Kulkarni RN, Postic C, et al.: Loss of insulin signaling in hepatocytes leads to severe insulin resistance and progressive hepatic dysfunction. *Mol Cell* 6:87–97, 2000
2. DeFronzo RA: Insulin resistance: a multifaceted syndrome responsible for NIDDM, obesity, hypertension, dyslipidaemia and atherosclerosis. *Neth J Med* 50:191–197, 1997
3. O'Brien RM, Granner DK: Regulation of gene expression by insulin. *Physiol Rev* 76:1109–1161, 1996
4. Lizcano JM, Alessi DR: The insulin signalling pathway. *Curr Biol* 12:R236–R238, 2002
5. Barthel A, Schmoll D: Novel concepts in insulin regulation of hepatic gluconeogenesis. *Am J Physiol Endocrinol Metab* 285:E685–E692, 2003
6. Shulman GI: Cellular mechanisms of insulin resistance. *J Clin Invest* 106:171–176, 2000
7. Kobayashi K: Adipokines: therapeutic targets for metabolic syndrome. *Curr Drug Targets* 6:525–529, 2005
8. Taniguchi CM, Emanuelli B, Kahn CR: Critical nodes in signalling pathways: insights into insulin action. *Nat Rev Mol Cell Biol* 7:85–96, 2006
9. Ozcan U, Cao Q, Yilmaz E, et al.: Endoplasmic reticulum stress links obesity, insulin action, and type 2 diabetes. *Science* 306:457–461, 2004
10. Schroder M, Kaufman RJ: ER stress and the unfolded protein response. *Mutat Res* 569:29–63, 2005
11. Ron D, Walter P: Signal integration in the endoplasmic reticulum unfolded protein response. *Nat Rev Mol Cell Biol* 8:519–529, 2007
12. Gregor MG, Hotamisligil GS: Adipocyte stress: the endoplasmic reticulum and metabolic disease. *J Lipid Res* 48:1905–1914, 2007
13. Ji C, Kaplowitz N: ER stress: can the liver cope? *J Hepatol* 45:321–333, 2006
14. Elchebly M, Payette P, Michaliszyn E, et al.: Increased insulin sensitivity and obesity resistance in mice lacking the protein tyrosine phosphatase-1B gene. *Science* 283:1544–1548, 1999
15. Klaman LD, Boss O, Peroni OD, et al.: Increased energy expenditure, decreased adiposity, and tissue-specific insulin sensitivity in protein-tyrosine phosphatase 1B-deficient mice. *Mol Cell Biol* 20:5479–5489, 2000
16. Gu F, Nguyen DT, Stuible M, et al.: Protein-tyrosine phosphatase 1B potentiates IRE1 signaling during endoplasmic reticulum stress. *J Biol Chem* 279:49689–49693, 2004
17. Lam TK, Pocai A, Gutierrez-Juarez R, et al.: Hypothalamic sensing of circulating fatty acids is required for glucose homeostasis. *Nat Med* 11:320–327, 2005
18. Bence KK, Delibegovic M, Xue B, et al.: Neuronal PTP1B regulates body weight, adiposity and leptin action. *Nat Med* 12:917–924, 2006
19. Delibegovic M, Bence KK, Mody N, et al.: Improved glucose homeostasis in mice with muscle-specific deletion of protein-tyrosine phosphatase 1B. *Mol Cell Biol* 27:7727–7734, 2007
20. Zabolotny JM, Haj FG, Kim YB, et al.: Transgenic overexpression of protein-tyrosine phosphatase 1B in muscle causes insulin resistance, but overexpression with leukocyte antigen-related phosphatase does not additively impair insulin action. *J Biol Chem* 279:24844–24851, 2004
21. Folch J, Lees M, Sloane Stanley GH: A simple method for the isolation and purification of total lipids from animal tissues. *J Biol Chem* 226:497–509, 1957
22. Morrison WR, Smith LM: Preparation of fatty acid methyl esters and dimethylacetals from lipids with boron fluoride–methanol. *J Lipid Res* 5:600–608, 1964
23. Rudel LL, Kelley K, Sawyer JK, et al.: Dietary monounsaturated fatty acids promote aortic atherosclerosis in LDL receptor-null, human ApoB100-overexpressing transgenic mice. *Arterioscler Thromb Vasc Biol* 18:1818–1827, 1998
24. Salmeen A, Andersen JN, Myers MP, et al.: Molecular basis for the dephosphorylation of the activation segment of the insulin receptor by protein tyrosine phosphatase 1B. *Mol Cell* 6:1401–1412, 2000
25. Haj FG, Zabolotny JM, Kim YB, et al.: Liver-specific protein-tyrosine phosphatase 1B (PTP1B) re-expression alters glucose homeostasis of PTP1B$^{-/-}$mice. *J Biol Chem* 280:15038–15046, 2005
26. Horton JD, Goldstein JL, Brown MS: SREBPs: Activators of the complete program of cholesterol and fatty acid synthesis in the liver. *J Clin Invest* 109:1125–1131, 2002
27. Brown MS, Goldstein JL: Selective versus total insulin resistance: a pathogenic paradox. *Cell Metab* 7:95–96, 2008
28. Biddinger SB, Kahn CR: From mice to men: insights into the insulin resistance syndromes. *Annu Rev Physiol* 68:123–158, 2006
29. Biddinger SB, Hernandez-Ono A, Rask-Madsen C, et al.: Hepatic insulin resistance is sufficient to produce dyslipidemia and susceptibility to atherosclerosis. *Cell Metab* 7:125–134, 2008
30. Goldstein BJ, Bittner-Kowalczyk A, White MF, et al.: Tyrosine dephosphorylation and deactivation of insulin receptor substrate-1 by protein-tyrosine phosphatase 1B: possible facilitation by the formation of a ternary complex with the Grb2 adaptor protein. *J Biol Chem* 275:4283–4289, 2000
31. Taniguchi CM, Ueki K, Kahn R: Complementary roles of IRS-1 and IRS-2 in the hepatic regulation of metabolism. *J Clin Invest* 115:718–727, 2005
32. Daitoku H, Yamagata K, Matsuzaki H, et al.: Regulation of PGC-1 promoter activity by protein kinase B and the forkhead transcription factor FKHR. *Diabetes* 52:642–649, 2003
33. Southgate RJ, Bruce CR, Carey AL, et al.: PGC-1alpha gene expression is down-regulated by Akt-mediated phosphorylation and nuclear exclusion of FoxO1 in insulin-stimulated skeletal muscle. *FASEB J* 19:2072–2074, 2005
34. Puigserver P, Spiegelman BM: Peroxisome proliferator-activated receptor-gamma coactivator 1 alpha (PGC-1 alpha): transcriptional coactivator and metabolic regulator. *Endocr Rev* 24:78–90, 2003
35. Puigserver P, Rhee J, Donovan J, et al.: Insulin-regulated hepatic gluconeogenesis through FOXO1-PGC-1alpha interaction. *Nature* 423:550–555, 2003
36. Shimomura I, Bashmakov Y, Horton JD: Increased levels of nuclear SREBP-1c associated with fatty livers in two mouse models of diabetes mellitus. *J Biol Chem* 274:30028–30032, 1999
37. Shimomura I, Matsuda M, Hammer RE, et al.: Decreased IRS-2 and increased SREBP-1c lead to mixed insulin resistance and sensitivity in livers of lipodystrophic and ob/ob mice. *Mol Cell* 6:77–86, 2000
38. Tobe K, Suzuki R, Aoyama M, et al.: Increased expression of the sterol regulatory element-binding protein-1 gene in insulin receptor substrate-2$^{-/-}$ mouse liver. *J Biol Chem* 276:38337–38340, 2001
39. Cohen SE, Kokkotou E, Biddinger SB, et al.: High circulating leptin receptors with normal leptin sensitivity in liver-specific insulin receptor knock-out (LIRKO) mice. *J Biol Chem* 282:23672–23678, 2007
40. Ceddia RB, Koistinen HA, Zierath JR, et al.: Analysis of paradoxical observations on the association between leptin and insulin resistance. *FASEB J* 16:1163–1176, 2002
41. Wang JL, Chinookoswong N, Scully S, et al.: Differential effects of leptin in regulation of tissue glucose utilization in vivo. *Endocrinology* 140:2117–2124, 1999
42. Waring JF, Ciurlionis R, Clampit JE, et al.: PTP1B antisense-treated mice show regulation of genes involved in lipogenesis in liver and fat. *Mol Cell Endocrinol* 203:155–168, 2003
43. Shimizu S, Ugi S, Maegawa H, et al.: Protein-tyrosine phosphatase 1B as new activator for hepatic lipogenesis via sterol regulatory element-binding protein-1 gene expression. *J Biol Chem* 278:43095–43101, 2003
44. Gu F, Dube N, Kim JW, et al.: Protein tyrosine phosphatase 1B attenuates growth hormone-mediated JAK2-STAT signaling. *Mol Cell Biol* 23:3753–3762, 2003
45. Tollet-Egnell P, Parini P, Stahlberg N, et al.: Growth hormone-mediated alteration of fuel metabolism in the aged rat as determined from transcript profiles. *Physiol Genomics* 16:261–267, 2004
46. Ginsberg HN: Is the slippery slope from steatosis to steatohepatitis paved with triglyceride or cholesterol? *Cell Metab* 4:179–181, 2006
47. Mari M, Caballero F, Colell A, et al.: Mitochondrial free cholesterol loading sensitizes to TNF- and fas-mediated steatohepatitis. *Cell Metab* 4:185–198, 2006
48. Zabolotny JM, Kim YB, Welsh LA, et al.: Protein-tyrosine phosphatase 1B expression is induced by inflammation in vivo. *J Biol Chem* 283:14230–14241, 2008
49. Pei Z, Liu G, Lubben TH, et al.: Inhibition of protein tyrosine phosphatase 1B as a potential treatment of diabetes and obesity. *Curr Pharm Des* 10:3481–3504, 2004